Journal of Statistical Physics, Vol. 84, Nos. 1/2, 1996

Diffusion on Random Lattices

F. Wang[1,2] and E. G. D. Cohen[1]

Received July 14, 1995; final October 27, 1995

We study the motion of a point particle along the bonds of a two-dimensional random lattice, whose sites are randomly occupied with right and left rotators, which scatter the particle according to deterministic scattering rules. We consider both a Poisson (PRL) and a vectorized random lattice (VRL) and fixed as well as flipping scatterers. On both lattices, for fixed scatterers and equal concentrations of right and left rotators the same anomalous diffusion of the particle is obtained as before for the triangular lattice, where the mean square displacement is $\sim t$, the diffusion process non-Gaussian, and the particle trajectories exhibit scaling behavior as at a percolation threshold. For unequal concentrations the particle is trapped exponentially rapidly. This system can be considered as an extreme case of the Lorentz lattice gases on regular lattices discussed before or as an example of the motion of a particle along cracks or (grain or cellular) boundaries on a two-dimensional surface.

KEY WORDS: Random lattice; diffusion; critical behavior; hyperscaling; propagation; cellular boundaries.

1. INTRODUCTION

Random lattices have been considered for a number of years to discretize a system without introducing the spatial anisotropy associated with regular lattices. They have figured in a large number of applications including quantum field theory,[1] grain mosaics,[2] and also foams.[3] We will confine ourselves in this paper to two-dimensional lattices.

On the other hand, they also represent an extreme case for the motion of a particle on a regular lattice as in the (two-dimensional) Lorentz lattice

[1] Rockefeller University, New York, New York 10021.

[2] Permanent address: DCRC Research Park, University of Missouri-Columbia, Columbia, Missouri 65211.

0022-4715/96/0700-0233$09.50/0

gas cellular automata (LLGCA) studied before[4-7] in that a maximum homogeneity of the possible velocity directions of the particle occurs, closest to those found in a continuous gas. In LLGCA a point particle moves on a lattice whose sites are (partially or fully) randomly occupied by scatterers which deflect the velocity of the moving particle according to given deterministic scattering rules. In this paper, we will consider LLGCA on two random lattices, with left or right rotators as scatterers, which deflect the particle velocity in a direction which makes the largest possible angle with its incoming velocity (Fig. 1). This was done in order to make a comparison with the regular triangular lattice possible, where a similar choice was made.

The motion of the particle in these models can be considered as explorations of the motion of a particle along randomly distributed lines or grooves on a surface such as cracks or cellular boundaries, or alternatively as the behavior of LLGCA on a random lattice. The scattering rules we choose enable a direct comparison with the behavior of previous LLGCA on regular lattices; although indicative, they may not be the most natural ones for the motion along cracks or boundaries. We include some results for probabilistic scattering rules corresponding to our rotator model on a

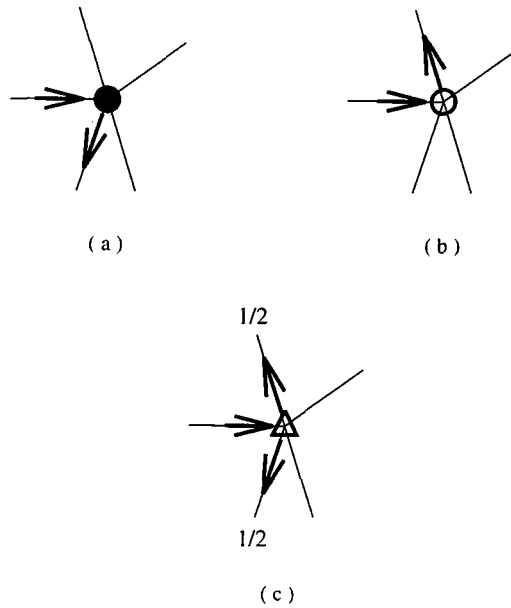

Fig. 1. Scattering rules for a rotator on a random lattice (Figs. 5a–5b): (a) right rotator (●); (b) left rotator (○); (c) probabilistic scattering rule (△).[12]

fully occupied random lattice. Then the particle has probability γ_L to turn to its left over the largest possible scattering angle and probability γ_R to turn to its right over the largest possible scattering angle. Since the particle has to turn either to the left or to the right, $\gamma_L + \gamma_R = 1$. In our computer simulations we chose $\gamma_L = \gamma_R = 1/2$ (Fig. 1c).

In Section 2 we discuss the construction of the two random lattices considered here: the Poisson random lattice (PRL) and the vectorized random lattice (VRL). In Section 3 we specify the two kinds of (rotator) scattering rules for which the motion of the particle over the random lattices is studied: fixed and flipping rotators; while Section 4 specifies the computer simulations and the physical quantities determined in them. Section 5 discusses the results obtained for fixed rotators, Section 6 those for flipping rotators. Section 7 comments on some of the results obtained.

2. CONSTRUCTION OF RANDOM LATTICES

An extensively used type of random lattice is the Delaunay random lattice,[1,8] which is an isotropic triangulation of a plane based on a given set of N random points in the plane. The Delaunay random lattice is easiest defined as the dual lattice to the Voronoi tessellation of the plane. The Voronoi construction or tessellation for a given set of points is defined as follows (Fig. 2): for all N random points we determine for each point (e.g. point P in Fig. 2) the associated cell consisting of the region of the plane nearer to this point than to any other point (*GHIJK* in Fig. 2). Whenever two cells share an edge they are considered as neighbors (e.g., the edge *JK* of the cells associated with P and A). By drawing a link (PA) between the two points associated with these cells one obtains a triangulation of the plane which is called the Delaunay lattice. This can be considered as a dual transformation from the Voronoi tessellation to the Delaunay random

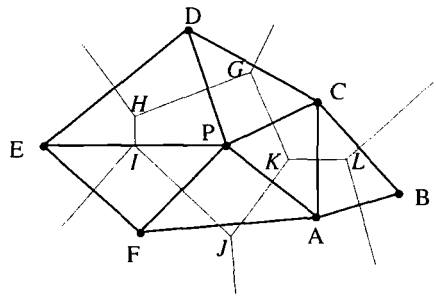

Fig. 2. Dual transformation between Delaunay random lattice (thick solid lines) and Voronoi tessellation (cells) (thin solid lines). Points A,..., F, P are the Delaunay random lattice sites; G, H,..., K belong to the Voronoi tessellation.

lattice in the sense that points of the Delaunay lattice (e.g., P) correspond to cells (e.g., *GHIJK*), links (e.g., PA) to cell edges (e.g., *JK*), and triangles (e.g., PAC) to vertices (e.g., *K*) of the Voronoi tessellation, respectively.

We will consider two Delaunay random lattices each constructed by connecting randomly distributed points on the plane with bonds (links), leading to a triangulation of the plane. Either we distribute the points randomly over the infinite plane, as described above, in which case a Poisson random lattice (PRL) (since the number of lattice points in a given volume is then a random variable with a Poisson distribution), introduced by Christ *et al.*[1] is obtained, or we first cover the plane with a regular square lattice and then distribute points randomly and homogeneously inside each square, such that each square contains only one point (Fig. 3a). In this case a vectorizable random lattice (VRL), introduced by Moukarzel and Herrmann,[9] is obtained, which allows a vectorizable (i.e., parallel) computer program for obtaining relevant properties of the lattice.

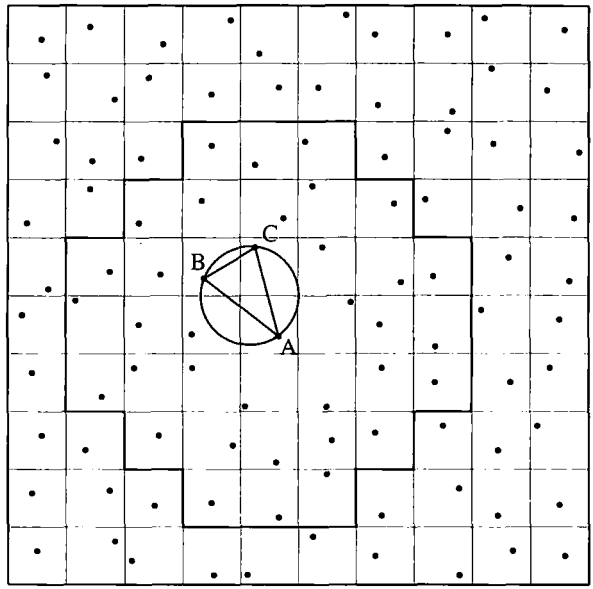

(a)

Fig. 3. (a) The division into squares in order to obtain the VRL. The points ● are randomly and homogeneously distributed inside each square of a square reference lattice. Also shown is the initial triangle *ABC* together with the 36-square neighborhood (thick solid line) of the initial point *A*; (b) probabilities for a point (e.g., *A*) to be connected to another point in the 36-square neighborhood; see ref. 9.

		4.12×10^{-5}	1.45×10^{-5}	4.12×10^{-5}		
	8.06×10^{-5}	1.56×10^{-2}	4.06×10^{-2}	1.56×10^{-2}	8.06×10^{-5}	
4.12×10^{-5}	1.56×10^{-2}	4.93×10^{-1}	9.36×10^{-1}	4.93×10^{-1}	1.56×10^{-2}	4.12×10^{-5}
1.45×10^{-5}	4.06×10^{-2}	9.36×10^{-1}	• A	9.36×10^{-1}	4.06×10^{-2}	1.45×10^{-5}
4.12×10^{-5}	1.56×10^{-2}	4.93×10^{-1}	9.36×10^{-1}	4.93×10^{-1}	1.56×10^{-2}	4.12×10^{-5}
	8.06×10^{-5}	1.56×10^{-2}	4.06×10^{-2}	1.56×10^{-2}	8.06×10^{-5}	
		4.12×10^{-5}	1.45×10^{-5}	4.12×10^{-5}		

(b)

Fig. 3. (*continued*)

2.1. Construction of PRL

We first describe a computer algorithm for generating a Delaunay random lattice consisting of points with uniformly distributed x and y coordinates. We start by putting points randomly in the plane. Then we choose an arbitrary point A (Fig. 4) and search out its nearest neighbor B. The two points $A$and B are linked. We then proceed as follows in order to find a triangle having this link as one of its sides: we note that each link can belong to two triangles, one on each side of the link, and that if we are given the link with its two endpoints and a side is chosen, it is straightforward to locate the third point of the triangle on that side. A way to do this is shown in Fig. 4. A circle is drawn through the endpoints of the link AB, its center being the link's midpoint M_1 (there is no point inside this circle, since B is the nearest neighbor of A). One then moves the center of the circle with points A and B on the circle by a small amount, dependent on the density of points, in the direction perpendicular to AB, where the next neighbor could be located, until one or more points are inside the circle with center M_3 (e.g., C_1 and C_2). One chooses then the point (C_1)

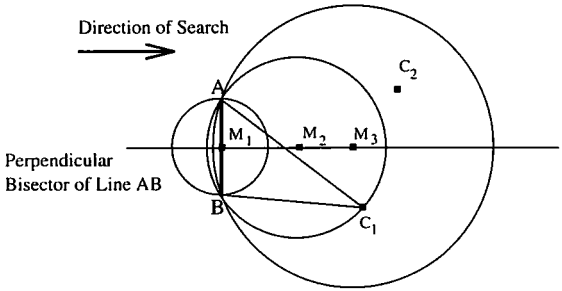

Fig. 4. Finding a new point in order to construct a new triangle starting from one link AB. Here M_1, M_2, and M_3 are centers of the circles located on one side of the perpendicular bisector of AB. Triangle ABC_1 is the first triangle; C_2 is a point of the random lattice which will be connected later.

giving rise to the circle with the smallest radius (i.e., with center M_2). In this way, we obtain the first triangle ABC_1.

The above procedure can then be repeated to link up the entire lattice. Starting with the triangle that has been completed, there are three links. We may now erect triangles on the other side of each link in the same way as described above. In this way we proceed from links to triangles and from triangles to new links. To avoid repetition, we keep a list of "active" links, i.e., those for which only one triangle has been found. When a new triangle is erected; we put each new link on the "active" list, unless it was already there in which case we remove it (which means that we already found the third point on both sides of that link). We also remove the old link from the active list. Each active link carries a tag that shows which side the known triangle is on. We erect triangles only on the "unknown" side of active links. When the active list is empty, all the links and triangles have been found and the Delaunay random lattice has been constructed. A part of a PRL is shown in Fig. 5a.

From the numerical point of view this approach is disadvantageous because there are no regularities of the lattice which can be used to substantially improve the performance of the simulation. This prevents the performance of large-scale simulations on the PRL. The reason is of course the lack of parallelism due to the fact that each lattice site has different characteristics, such as the number and relative location of the nearest neighbors of a given site. In fact, for the PRL the number of nearest neighbors of a site is not even bounded, because any spatial distribution of points is in principle possible. So, in order to introduce some regularities in the neighborhoods of the sites in the sense that, given any site, one has a simple rule to know which are its relevant neighbors, we consider also the VRL.

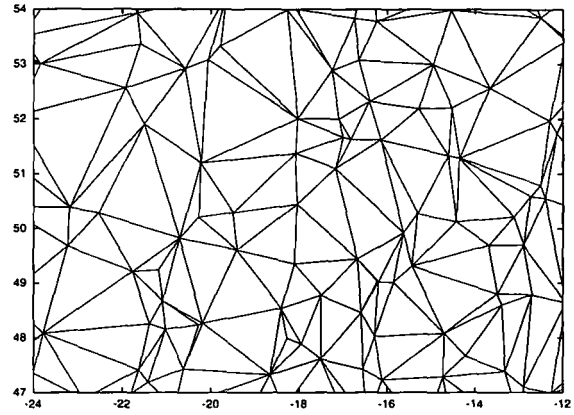

(a)

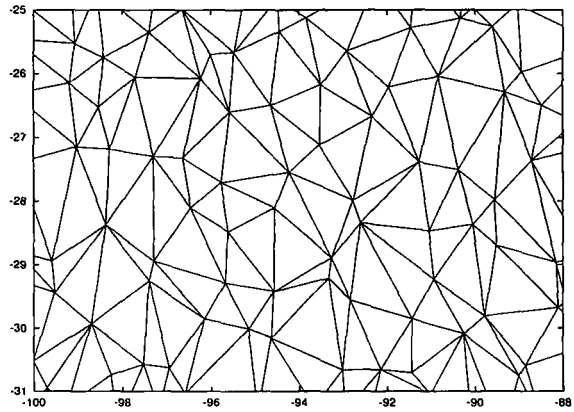

(b)

Fig. 5. Part of (a) a PRL; (b) a VRL.

2.2. Construction of VRL

The construction we describe closely follows the procedure described in ref. 9. We first define a regular lattice (here a square lattice), which we call the reference lattice. Next we randomly pick in each square a point with uniform distribution (Fig. 3a). These will be the sites of our VRL. The spatial distribution of these points is homogeneous, i.e., the probability to find a point at any position in the lattice is constant.

Unlike for the PRL, where a point can in principle be connected to any other point, here each point can only be connected to points in a 36-square neighborhood, as shown in Fig. 3a. So if a point belongs to a triangle, the other two points must be in two of the squares of this neighborhood. For, if one of these two points is *outside* this neighborhood, the circle defined by the three points so chosen will include at least one point *inside* the 36-square neighborhood. Therefore, to find a triangle one only has to search for neighboring points in this restricted area. An upper limit for the distance two neighboring points can have is $(4^2+2^2)^{1/2} = (20)^{1/2} \approx 4.472$, as can be seen in Fig. 3a.

The last step is to find the third point of the triangle: the probability to find this point is not equal for all squares in the neighborhood of a given square, but is much smaller for the outer squares. In Fig. 3b the numerically determined probabilities for the center point to be connected to another to point in this neighborhood are shown.[9] So we begin the search for the third point in those squares which have the highest probability (Figs. 3a, 3b) and then going outward to the squares with lower probability, possibly cutting off the search at outer squares with probabilities $< 10^{-3}$. A part of a VRL is shown in Fig. 5b.

2.3. Isotropy

The probability that a site located at the origin has a neighbor at the point (r, θ) in polar coordinates provides a measure for isotropy. If the local properties of the lattice were fully isotropic, no θ dependence would be obtained. This is indeed so for the PRL, but for the VRL, the probability shows some mild anisotropy.[9] This is of course not surprising, since the reference lattice was anisotropic; so even though the distribution of single lattice points is itself homogeneous in space, the probability for pairs of lattice points has a weak anisotropic bias.[9]

3. ROTATOR MODEL

Since straight lines may pass through some but not all lattice sites on the random lattice, only the case of a fully occupied random lattice whose sites are all occupied by scatterers, i.e., with concentration of scatterers $C = 1$, has been considered, since otherwise a model with two different types of scattering rules would have to be introduced. We chose the time step = the particle speed = 1. However, unlike the regular lattices considered previously, the lattice distances on a random lattice differ from lattice site to lattice site. Therefore, during one time step, there is no collision with a scatterer if the lattice distance is longer than 1 and there is

one or more than one collision with a scatterer if the lattice distance is shorter than 1. This causes no difference, however, in the diffusive behavior. Choosing, e.g., variable particle speeds so that the particle would always travel between two adjacent lattice sites in a time step would not change our results.

In our rotator model, the particle turns to its left (right) over the largest available angle between the incoming and outgoing velocity directions (Figs. 1a and 1b). The right and left rotators are randomly distributed over the sites of the random lattice and the fraction of lattice sites occupied by right (left) rotators will be denoted by $C_R(C_L)$, so that $C = C_R + C_L = 1$.

An analytical treatment of the motion of a particle on the random lattice occupied by rotators is very difficult. Not only is it not obvious how to write down the microscopic equations of motion for the moving particle, but, in addition, even if one did, the equations of motion could essentially only conveniently be solved at present in the Boltzmann approximation, which does not give meaningful results for this nondilute deterministic lattice gas.[11] Therefore we will only describe the computer program we used to study numerically the diffusive motion of the particle through the scatterers over the lattice. Before we do so, we note that we consider two kinds of (right and left) rotator models: fixed and flipping. Fixed rotators are not only fixed in position during the entire motion of the particle, but also as to their (right or left scattering) state, while flipping rotators only have fixed positions, but change (flip) in state instantaneously from right to left rotator or vice versa, after a collision with the particle has occurred.

We remark that for fixed scatterers the diffusive behavior of one moving particle or of many simultaneously moving but mutually noninteracting particles is the same, since the particles move through the scatterers independently of each other. However, this is not true for the flipping scatterers, where the change in character of the scatterer after a collision with a particle introduces an indirect interaction between the particles via the scatterers and vice versa.

4. COMPUTER SIMULATIONS

A similar computer algorithm is used here for the two random lattices as was used before for the quasi-lattice,[7] except that strictly periodic boundary conditions could be employed here. The basic unit cell is a square containing 10,000 lattice sites and the periodic boundary conditions are defined as follows: if no more points can be found on one side of a link because one is close to a boundary of the unit cell, the points (x, y) inside the unit cell from the opposite boundary are moved by the transformation $(x \pm 100, y)$ or $(x, y \pm 100)$ outside the unit cell to generate the next cell of

the checkerboard which will ultimately form the random lattice by repetition of this procedure.

We are interested in the diffusive behavior of the moving particle due to the scatterers. To that end, we studied the following quantities:

1. The mean square displacement $\Delta(t) \equiv \langle |\mathbf{r}(t)|^2 \rangle = \langle r^2(t) \rangle$, where $\mathbf{r}(t)$ and $r(t)$ are the displacement and distance of the particle position at time t from its initial position at time $t=0$, respectively, with $r(t) = |\mathbf{r}(t)|$ and the average $\langle \cdot \rangle$ taken over all random configurations of the scatterers over the lattice.

2. From $\Delta(t)$, we can define a time-dependent diffusion coefficient $D(t) = \Delta(t)/4t$. If $D(t)$ approaches a finite limit when $t \to \infty$, this limit is the diffusion coefficient constant D in the normal sense.

3. The kurtosis $K(t) \equiv \langle x^4(t) \rangle / \langle x^2(t) \rangle^2 - 3$, where $x(t)$ is the displacement along the x axis. Since for Gaussian diffusion $K(t) = 0$, $K(t) \neq 0$ indicates non-Gaussian diffusion. An even more detailed description of the diffusion process is given by the following:

4. The probability distribution function $P(\mathbf{r}, t)$, which gives the probability to find a particle at position $\mathbf{r}$ at time t if the particle is initially at $\mathbf{r} = 0$ when $t = 0$. In our computer simulations, we actually determine the radial probability distribution function

$$\hat{P}(r, t) = r \sum_{\theta=0}^{2\pi} P(\mathbf{r}, t) = r \sum_{\theta=0}^{2\pi} P(\mathbf{r}(r, \theta), t)$$

which is the probability to find a particle at r at t if the particle is initially at $r = 0$ when $t = 0$, where r and θ are the polar coordinates of $\mathbf{r}$.

5. FIXED ROTATORS

The simulation results indicate for both random lattices an absence of diffusion for all unequal concentrations $C_R \neq C_L$ of right and left rotators, since all particles then get trapped after a finite number of time steps. Thus the mean square displacement $\Delta(t)$ is bounded, so that $\Delta(t) \to \text{const}$ and $D(t)$ goes to zero as $1/t$ (Figs. 6a, 6b). Also, the radial probability distribution function $\hat{P}(r, t)$ no longer appears to change after $t \simeq 2^{10}$ (Figs. 6f, 6g). For equal concentrations $C_R = C_L = 1/2$ of right and left rotators, on the other hand, $\Delta(t) \sim t$, so that $D(t) \to \text{const}$ and a time independent of the diffusion coefficient D can be defined (Figs. 6a, 6b). However, the kurtosis $K(t)$ does not go to zero (Fig. 6c) and the radial probability distribution $\hat{P}(r, t)$ does not correspond to that of a Gaussian probability distribution (Figs. 6d–6e), a diffusive behavior called anomalous diffusion before.[4–7,12]

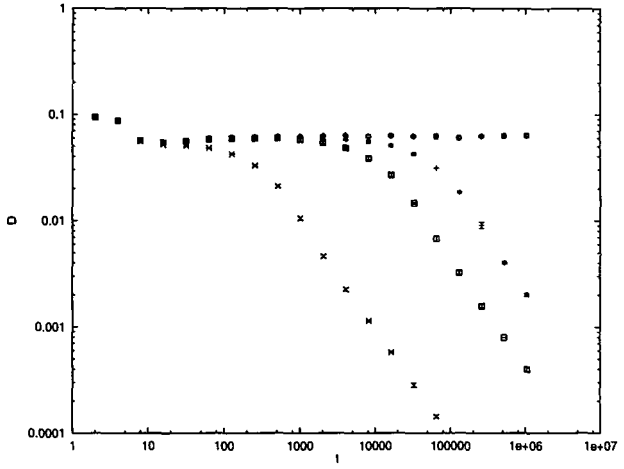

(a)

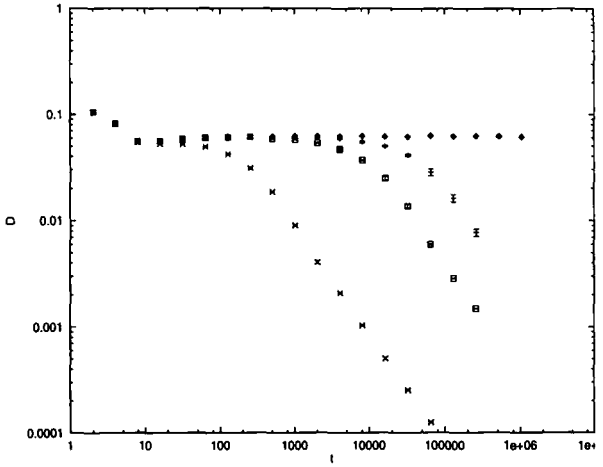

(b)

Fig. 6. Diffusion coefficient $D(t)$ as a function of t on a $\log_{10}$-$\log_{10}$ scale for the fixed rotator model $C_L = C_R = 0.5$ ($\diamond$) (approaching a constant), $C_L = 0.51$, $C_R = 0.49$ ($+$); $C_L = 0.52$, $C_R = 0.48$ ($\square$), and $C_L = 0.6$, $C_R = 0.4$ ($\times$) (these three curves have slopes of -1) on the (a) PRL and (b) VRL, respectively; (c) corresponding kurtosis $K(t)$ as a function of t for $C_L = C_R = 0.5$ on the PRL ($\diamond$) and the VRL ($+$); the radial probability distribution function $\hat{P}(r, t)$ as a function of r for the fixed rotator model at $t = 2^{10}$ ($\diamond$), $t = 2^{11}$ ($+$), and $t = 2^{12}$ ($\square$), respectively, for (d) $C_L = C_R = 0.5$ on the PRL, (e) $C_L = C_R = 0.5$ on the VRL, (f) $C_L = 0.6$, $C_R = 0.4$ on the PRL, and (g) $C_L = 0.6$, $C_R = 0.4$ on the VRL. Here as in the following figures, when the error bars are invisible, they are of the order of the symbol size.

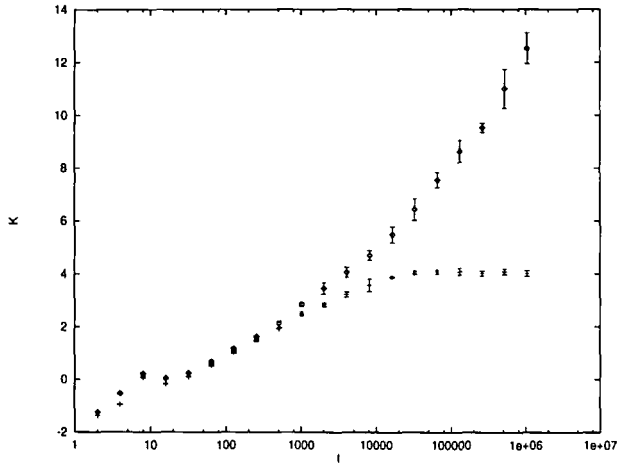

(c)

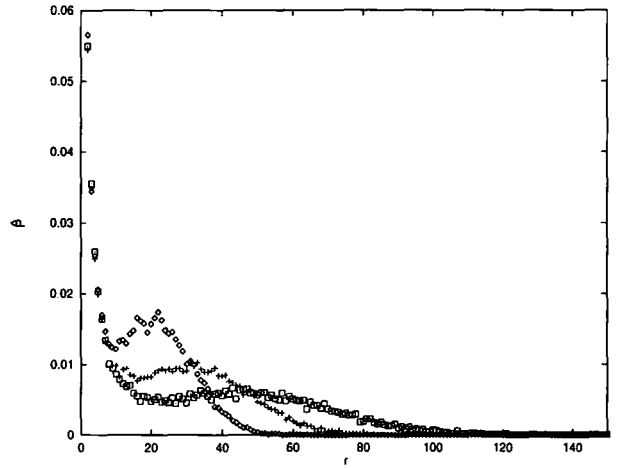

(d)

Fig. 6 (*continued*)

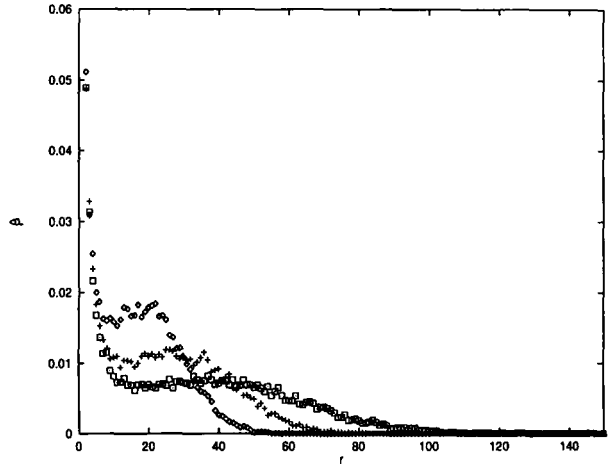

(e)

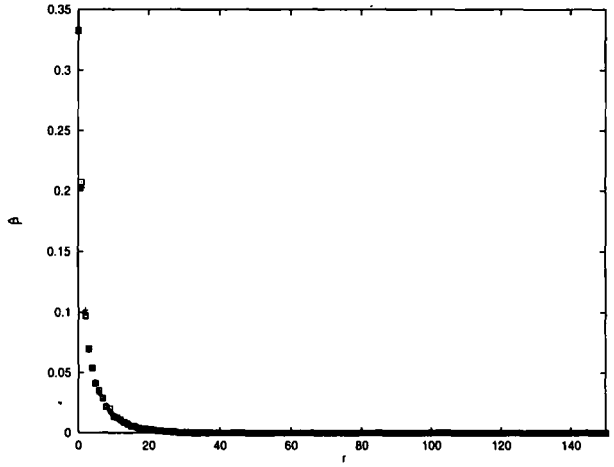

(f)

Fig. 6 (*continued*)

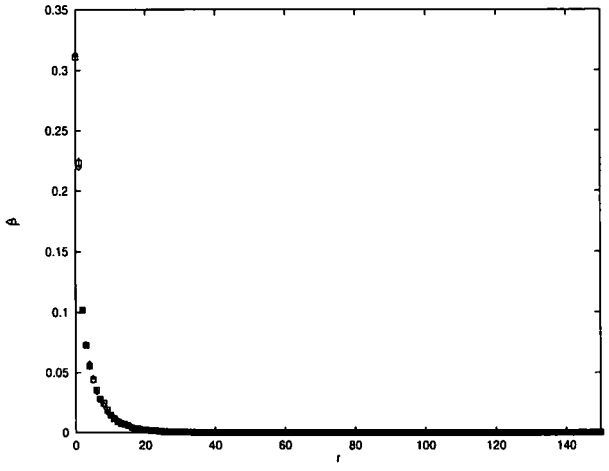

(g)

Fig. 6 (*continued*)

In this case, a critical or scaling behavior of the particle trajectories occurs characterized by exponents which are identical to those found for two-dimensional percolation clusters, without there being any connection here of the particle trajectories with such clusters, whose existence on random lattices is even less clear than on not fully occupied regular lattices.[4-7]

The scaling behavior at $C_R = C_L = 1/2$ on the random lattice is identical to that found for the rotator model on the triangular lattice and the absence of a connection with an associated percolation problem occurred there also for $C_R = C_L$ when $C < 1$ (as opposed to $C = 1$ here.)

Thus the number of particle trajectories still open (closed) at time t decreases (increases) as $t^{-1/7}$ for $C_R = C_L = 1/2$ (Fig. 7a), indicating that all trajectories will close eventually and the particle will move in a periodic orbit on the lattice. For $C_R \neq C_L \neq 1/2$, however, the number of open (closed) orbits decreases (increases) exponentially in time.

The critical behavior at $C_R = C_L = 1/2$ exhibits the same hyperscaling relation between the exponent τ associated with the lower cumulative probability $P_o(t)$ for the decay of open trajectories with time, $t^{-1/7} \sim t^{2-\tau}$ and the same fractal dimension d_f derived from the mean square displacement for such orbits, $\Delta_o(t) \sim t^{2/d_f}$, as on the triangular lattice:[4-7] $\tau - 1 = 2/d_f$ ($\tau = 15/7$, $d_f = 7/4$) (Fig. 7).

The similarity with the triangular lattice may be related to the fact that the average coordination number on the random lattice is 6, the same as

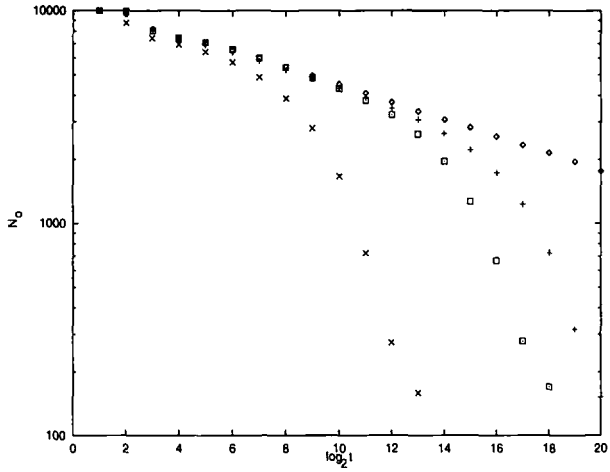

(a)

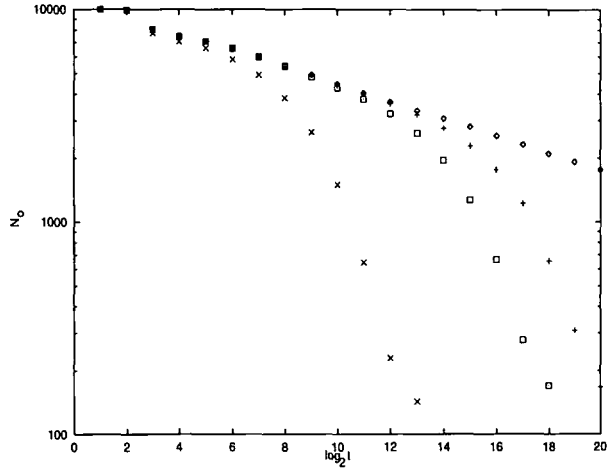

(b)

Fig. 7. The number of open orbits $N_o(t)$ out of 10,000 trajectories as a function of t on a $\log_{10}$–$\log_2$ scale for the fixed rotator model for $C_L = C_R = 0.5$ ($\diamond$) [the slope approaches $\sim -1/(7 \log_2 10)$], $C_L = 0.51$, $C_R = 0.49$ ($+$), $C_L = 0.52$, $C_R = 0.48$ ($\square$), and $C_L = 0.6$, $C_R = 0.4$ ($\times$) [these three curves decay exponentially] on the (a) PRL and (b) VRL; corresponding contributions to the diffusion coefficient from open orbits $P_o(t)\, \Delta_o(t)/t$ as a function of t on a $\log_{10}$–$\log_2$ scale for $C_L = C_R = 0.5$ ($\diamond$) (the slope approaches a constant), $C_L = 0.51$, $C_R = 0.49$ ($+$) and $C_L = 0.52$, $C_R = 0.48$ ($\square$) (these two curves decay exponentially) on the (c) PRL and (d) VRL.

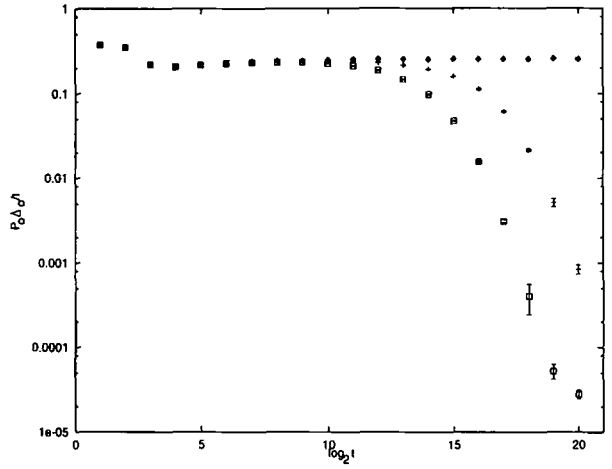

(c)

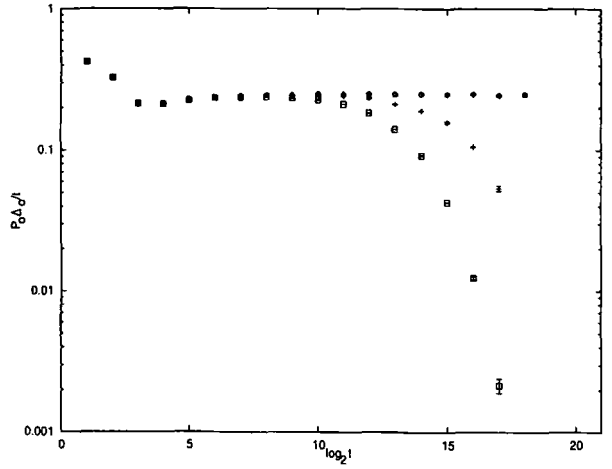

(d)

Fig. 7 (*continued*)

for the triangular lattice, and also that the random lattice is constructed as a triangulation of the plane.

The absence of effects due to the finite size of our basic cell and the efficacy of the periodic boundary conditions was confirmed by the virtually identical diffusive behavior found for a basic cell of 2500 instead of 10,000 lattice sites. However, the basic cell may well still be too small to discover possible logarithmic corrections, etc., to our results.[10]

6. FLIPPING ROTATORS

As on the not fully occupied triangular lattice for $0 < C < 1$ for flipping rotators,[4-7,12] the diffusive behavior is quasinormal on the PRL; it is, however, normal on the VRL.

6.1. On the PRL

For the PRL, although the diffusion coefficient and the kurtosis look like those for Gaussian diffusion (Figs. 8a, 8b), the radial distribution function $\hat{P}(r, t)$ clearly exhibits non-Gaussian behavior (Fig. 8c), since the points near the origin are due to periodic orbits. However, as the fraction of closed orbits is very small, the diffusion coefficient and kurtosis look like those for normal diffusion, so that we call this behavior quasinormal. A few examples of periodic orbits are shown in Figs. 9a–9c. Unlike on the triangular lattice, where only periodic orbits for $t < 2^6$ are found on the computer (Fig. 10a), there are much longer periodic orbits here (Figs. 9a–9c), yet the fraction of all periodic orbits is even smaller than on the triangular lattice; cf. the peak value (for periodic orbits) of 0.011 on the triangular lattice (Fig. 10b) with 0.001 on the PRL (Fig. 8c). Thus the overwhelming majority of trajectories remain open.

Since the random lattice is constructed as a triangulation of a plane, the motion of the particle on the fully occupied random lattice is similar to that on the triangular lattice. Now for the flipping rotator model on the fully occupied triangular lattice the particle always propagates to infinity, no matter what the concentrations C_L and C_R are.[4-7,12] On the random lattice the particle trajectories for the flipping rotator model have a similar propagating behavior as on the triangular lattice (Figs. 11a, 11b). However, because of the irregularity of the random lattice, the "propagation" in a particular direction cannot last long before another "propagation" starts in another direction, leading, after many such propagation direction changes to a randomized motion of the particle on the lattice. Thus, in spite of short term "propagations," the moving particle exhibits on the long time scale normal diffusion (except for a very small probability to make a

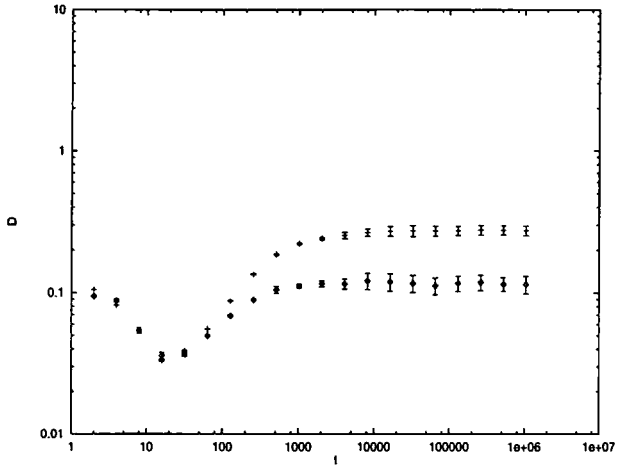

(a)

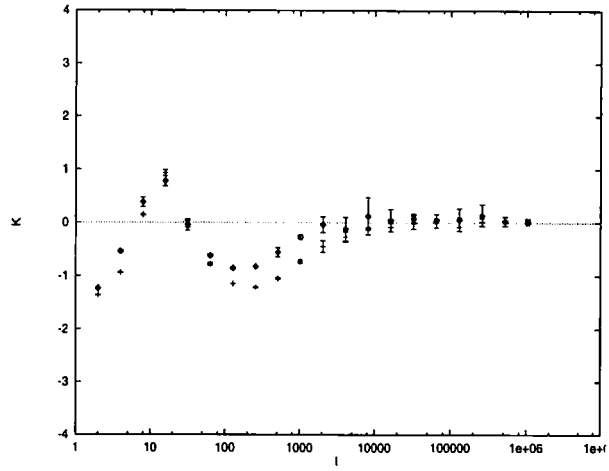

(b)

Fig. 8. (a) Diffusion coefficient $D(t)$ as a function of t on a $\log_{10}$–$\log_{10}$ scale for the flipping rotator model for $C_L = C_R = 0.5$ (approaching a constant) on the PRL ($\diamond$) and VRL ($+$); (b) corresponding kurtosis on the PRL ($\diamond$) and VRL ($+$); corresponding $\hat{P}(r, t)$ at $t = 2^{19}$ ($\diamond$) and $t = 2^{20}$ ($+$), respectively, on the (c) PRL and (d) VRL (note the very small values of $\hat{P}$). Only one typical error bar is shown at $r = 336$ in (c) and at $r = 303$ in (d), respectively, for clarity; solid lines are the $\hat{P}$ for the corresponding Gaussian distributions, using the measured value for the diffusion coefficient [note the presence of points representing periodic orbits near the origin in (c), but not for the VRL in (d)].

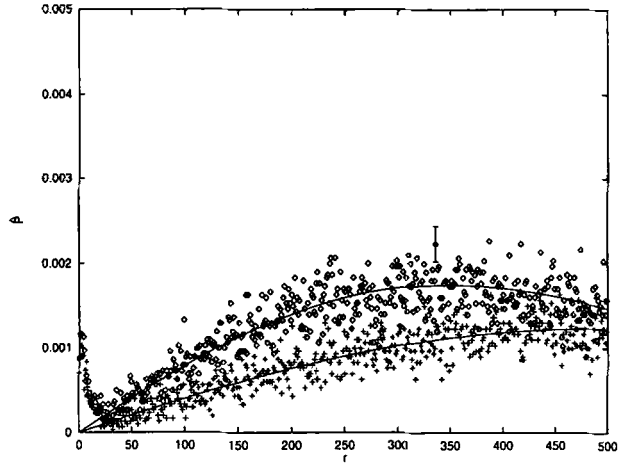

(c)

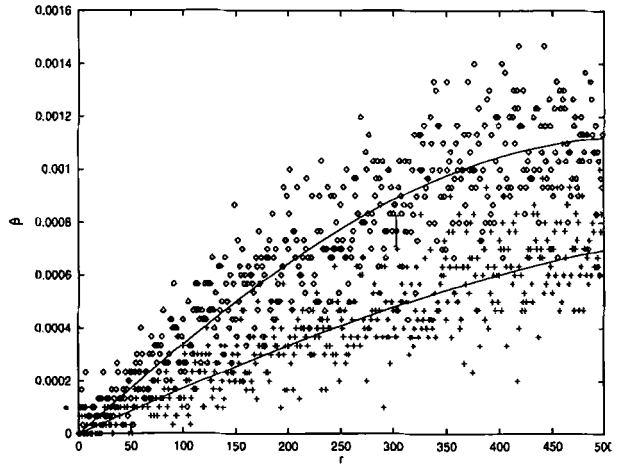

(d)

Fig. 8 (*continued*)

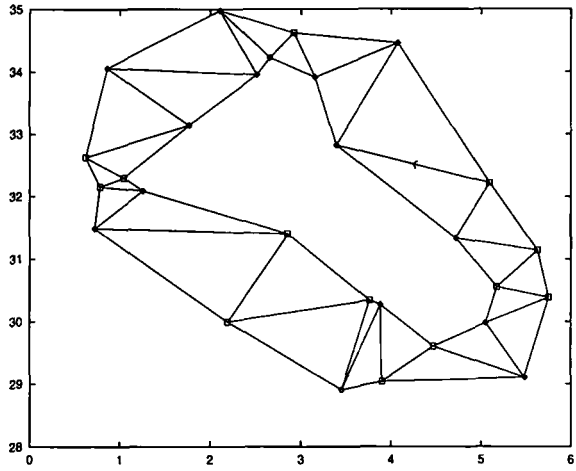

(a)

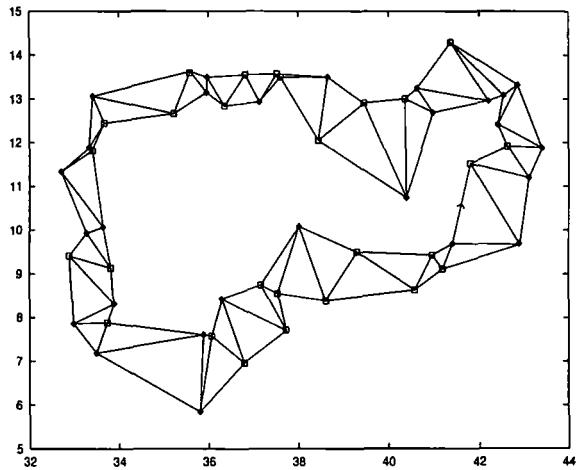

(b)

Fig. 9. Example of periodic orbits with (a) a period of 9176 time steps on 28 lattice sites, (b) a periodic orbit with a period of 4097 time steps on 54 lattice sites, and (c) a period of 318 time steps on 7 lattice sites, for the flipping rotator model on the PRL. The symbol □ stands for a right rotator, ◇ stands for a left rotator, and the arrows indicate the initial position and velocity direction.

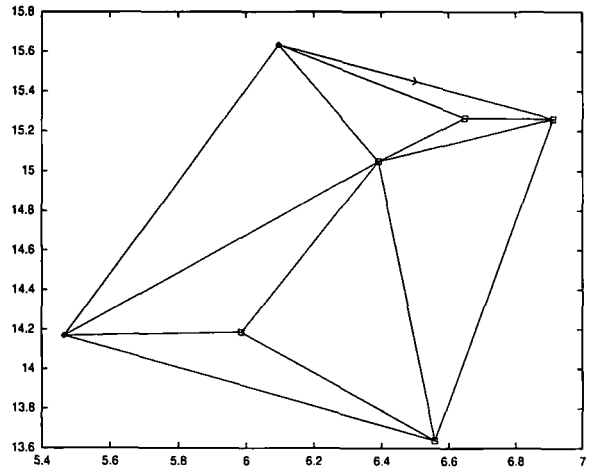

(c)

Fig. 9 (*continued*)

periodic orbit). This is as on the partially occupied triangular lattice, where the presence of randomly placed unoccupied lattice sites leads to a similar quasinormal diffusive behavior.[4–7] Since the particle spends a lot of time moving back and forth during each short term "propagation," (see Figs. 11a–11d), the diffusion coefficient is very small compared to that on the partially occupied triangular lattice (Fig. 10c), where this does not occur.

We note that even for the periodic orbits in Figs. 9a and 9b (not in Fig. 9c, which could be the smallest one, with only seven lattice sites), the particle orbit is composed of short term "propagations," except that the particle comes back to the origin with the same velocity and configuration of rotators as the initial one, leading to a periodic particle orbit.

6.2. On the VRL

For the VRL, no closed orbits have been found so far. The diffusion appears to be Gaussian, i.e., $\Delta(t) \sim t$, so that $D(t) \to \text{const}$ and $K(t) \to 0$ and $\hat{P}(r, t)$ is consistent with a Gaussian distribution (Figs. 8b–8d).

We note that the diffusion coefficient for the VRL is about three times larger than that of the PRL (Fig. 8a). We believe that this is due to (1) the structure of the VRL, which is more regular than that of the PRL, and leads to relatively longer "propagations" for the particle on the VRL than

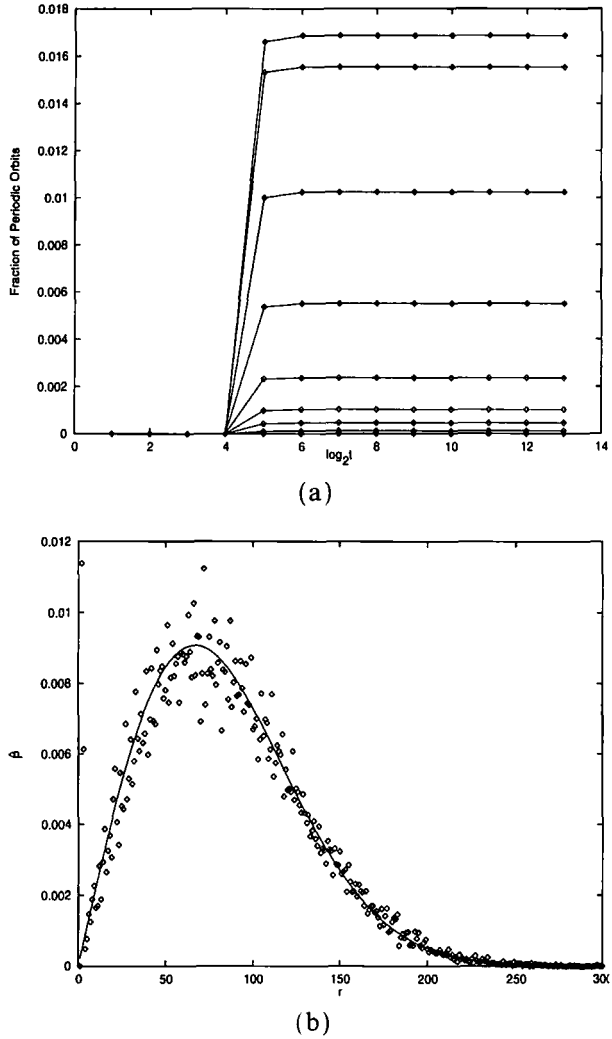

Fig. 10. (a) Fraction of periodic orbits for the flipping rotator model on the triangular lattice as a function of $\log_2 t$ for different concentrations of rotators for $C_L = C_R$; from top to bottom: $C = 0.85, 0.8, 0.7, 0.6, 0.5, 0.4, 0.3, 0.2, 0.1$ (the last two are too small to see), respectively; (b) corresponding $\hat{P}(r, t)$ for $C = 0.85$ and $C_L = C_R$ at $t = 2^{13}$; solid line is $\hat{P}$ for the corresponding Gaussian distribution (note the few points representing periodic orbits near the origin); (c) comparison of the diffusion coefficient D as a function of C for $C_L = C_R$ for the flipping rotator model on the triangular lattice ($\diamond$), which goes to infinity when the concentration $C \to 0$ or 1; on the PRL for $C_L = C_R = 0.5$ ($C = 1$) ($+$) with value ~ 0.11, on the VRL for $C_L = C_R = 0.5$ ($\square$) with value ~ 0.27, and the diffusion coefficient for a probabilistic model based on the rotator model on the PRL ($\times$) and VRL ($\triangle$) (these two are indistinguishable) for $C_L = C_R = 0.5$ ($\times$) with value ~ 0.038.

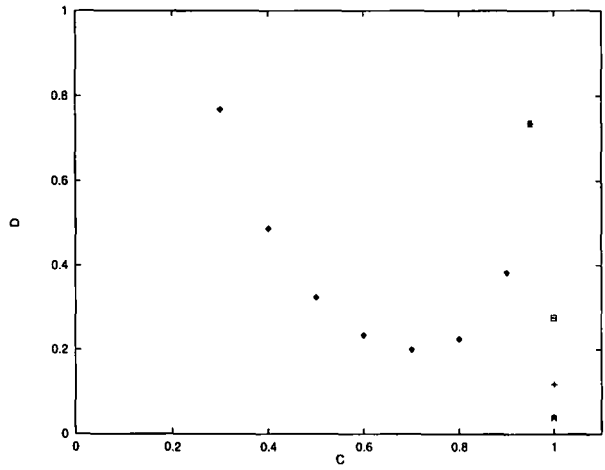

(c)

Fig. 10 (*continued*)

on the PRL (Figs. 11a–11d); and (2) the fact that there are no closed orbits on the VRL (Fig. 8d).

It is obvious that the first reason is dominant, since the number of closed orbits on the PRL is very small.

6.3. Comparison with the Probabilistic Scattering Rules

The quasinormal and normal diffusive behavior of the flipping rotator models on the PRL and VRL make a comparison with models with probabilistic scattering rules possible, since the computer simulation results indicate that the diffusive behavior of a particle moving through scatterers with probabilistic scattering rules, is always Gaussian. Because of the "propagations" that take place on both the PRL and the VRL, the diffusion coefficients on these lattices are larger than for a probabilistic model, which corresponds to the rotator model for $C_L = C_R = 1/2$, i.e., for a model with equal probability for the particle velocity direction to scatter over the largest angle to its right or its left at a given lattice site (Figs. 1c, 12a, 12b).

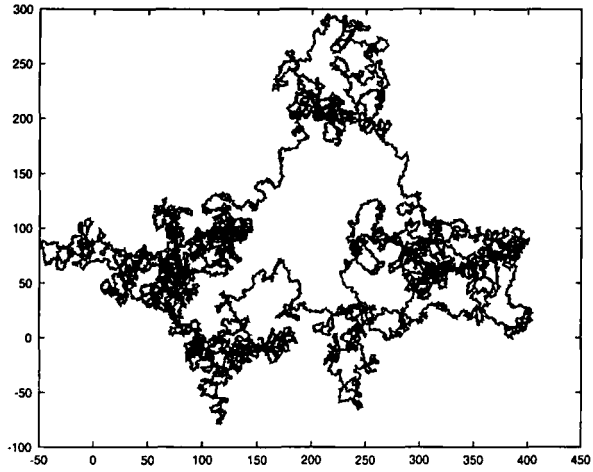

(a)

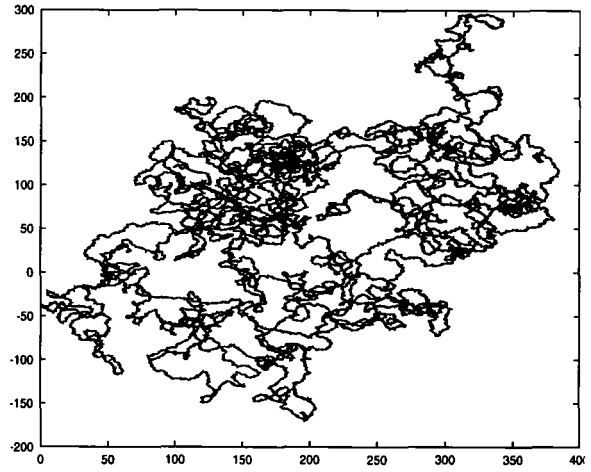

(b)

Fig. 11. Examples of particle trajectories for $C_L = C_R = 0.5$ and $t \simeq 100,000$ time steps for the flipping rotator model on the (a) PRL and (b) VRL; part of the trajectories (500 time steps) on the (c) PRL and (d) VRL, on which many short term (back and forth) propagations occur.

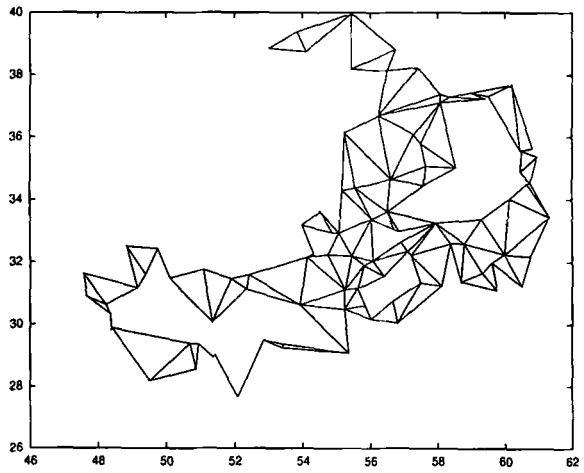

(c)

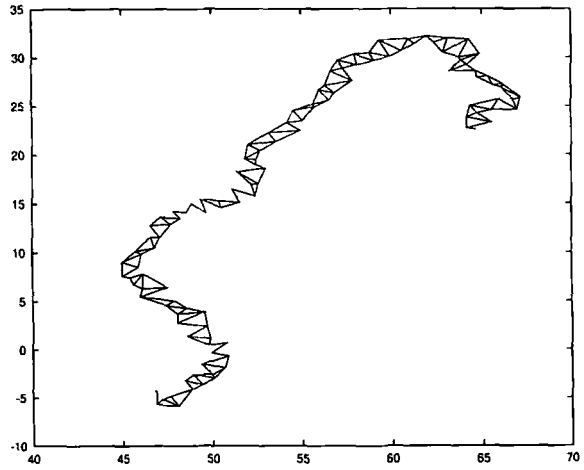

(d)

Fig. 11 (*continued*)

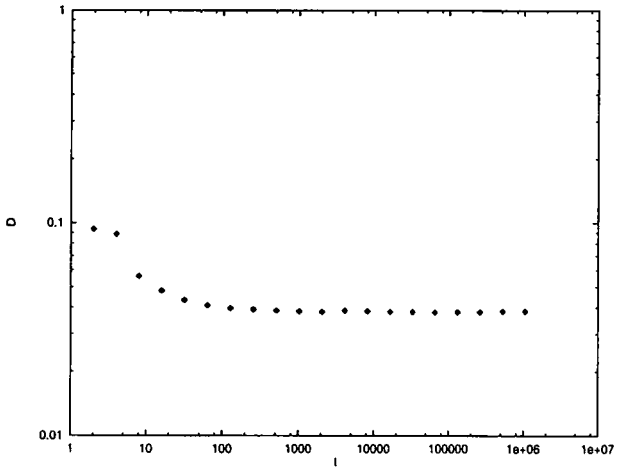

(a)

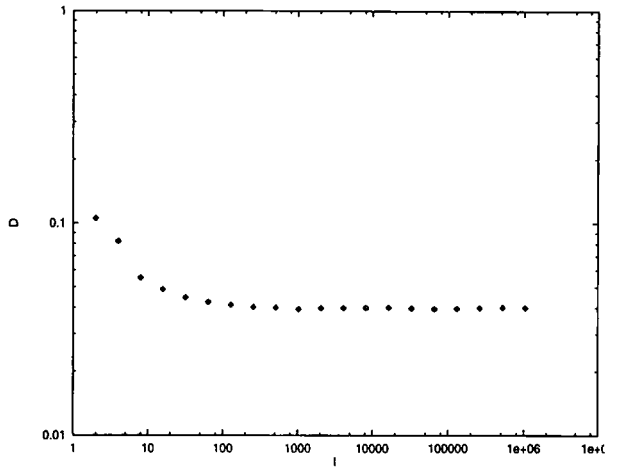

(b)

Fig. 12. Diffusion coefficient D as a function of time t on a $\log_{10}$–$\log_{10}$ scale for a probabilistic model based on the fixed rotator model for $C_L = C_R = 0.5$ on the (a) PRL and (b) VRL; corresponding particle trajectories of 100,000 time steps on the (c) PRL and (d) VRL.

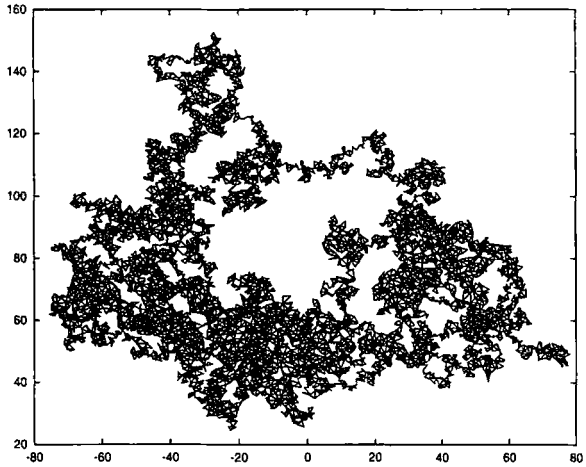

(c)

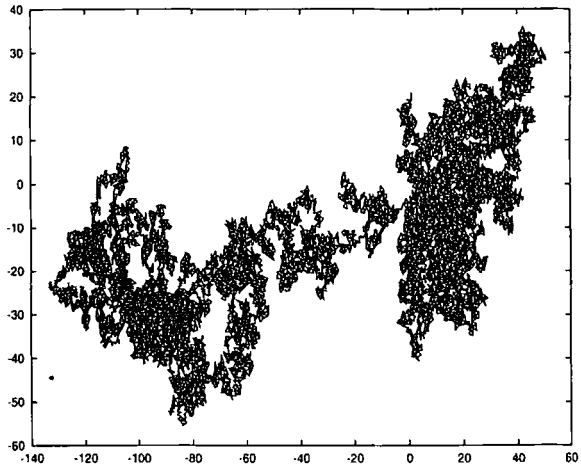

(d)

Fig. 12 (*continued*)

7. DISCUSSION

We conclude with a number of remarks.

1. The random lattices exhibit the same kinds of diffusive behavior as the regular lattices studied before.[4–7] Although the behavior can naturally be compared with that on a triangular lattice, it is also similar to that found for the square[4–7] and honeycomb[4–7] lattices for particular scattering rules and scatterer concentrations.

2. The most striking difference between the diffusive behavior on the two random lattices is for flipping rotators, where for the VRL no closed particle orbits have been found, while for the PRL a very small but finite number was seen. This might well be due to the slightly more regular structure of the VRL as compared to the PRL, which allows longer propagations than on the PRL (Figs. 11c and 11d) and also leads to a larger diffusion coefficient on the VRL than on the PRL (Fig. 8a). The difference in the particle motion on the PRL and VRL when deterministic or probabilistic scattering rules are used is shown in Figs. 11a, 11b and 12c, and 12d. One notices that the probabilistic motion gives rise to more densely space filling trajectories, because of the absence of propagation.

3. In so far as two-dimensional random lattice structures occur in nature or technology, it might be of interest to investigate other random lattices, as well as other scattering rules than those considered here, which were dictated to allow a comparison with those employed before on regular lattices. Such an investigation would address the question whether the same *universality* in scaling behavior of the trajectories observed before for regular lattices,[4–7] also obtains for random lattices in general. In particular, one could wonder whether such behavior is always found for an equal concentration of right and left rotators, independently of the nature of the random lattice or the scattering rule (e.g., whether scattering takes place over the largest or the smallest angle with the incoming velocity).

The fundamental difference between the diffusive behavior for probabilistic and deterministic scattering rules should, however, be kept in mind. For, while the first appears always to lead to normal, Gaussian, diffusion, the second exhibits a wide variety of behavior ranging from particle propagation to quick particle trapping in closed orbits.[4–7]

ACKNOWLEDGMENTS

The authors are indebted to Dr. M. Magnasco, for providing them with a computer program for the Poisson random lattice and a stimulating

discussion, as well as to Dr. H. C. Ren for many helpful discussions. E.G.D.C. gratefully acknowledges support from the U.S. Department of Energy under contract DE-FG02-88-ER13847.

REFERENCES

1. N. H. Christ, R. Friedberg, and T. D. Lee, *Nucl. Phys., B* **202**:89 (1982); R. Friedberg and H.-C. Ren, *Nucl. Phys. B* **235[FS11]**:310 (1984).
2. D. Weaire and N. Rivier, *Contempt. Phys.* **25**:59 (1984); N. Rivier, *Phil. Mag. B* **52**:795 (1985).
3. C. Moukarzel, *Physica A* **199**:19 (1993).
4. E. G. D. Cohen and F. Wang, New results for diffusion in Lorentz lattice gas cellular automata, *J. Stat. Phys.* **81**:445 (1995).
5. E. G. D. Cohen and F. Wang, Novel phenomena in Lorentz lattice gases, *Physica A* **219**:56 (1995).
6. F. Wang, Motion in Lorentz lattice gases, Ph.D. Thesis, Rockefeller University (1995).
7. F. Wang and E. G. D. Cohen, Diffusion in Lorentz lattice gas cellular automata: The honeycomb and quasi-lattices compared with the square and triangular lattices, *J. Stat. Phys.* **81**:467 (1995).
8. P. J. Grenn and R. Sibson, *Computer J.* **21**:168 (1977).
9. C. Moukarzel and H. J. Herrmann, *J. Stat. Phys.* **68**:911 (1992); C. Moukarzel, *Physica A* **190**:13 (1992).
10. M. Magnasco, *Phil. Mag. B* **69**:397 (1994).
11. G. A. van Velzen, Lorentz lattice gases, Ph.D. Thesis, University of Utrecht (1990).
12. X. P. Kong and E. G. D. Cohen, *J. Stat. Phys.* **63**:737 (1990).